A Simplified Production Method for Multimode Multisite Neuroprobes

K. Mankodiya[1], D. Krapohl[1], S. Hammad[1], Y. Xie[2], M. Klinger[3], U.G. Hofmann[1]
[1] Institute for Signal Processing, University of Luebeck, Luebeck, Germany
[2] Graduate School for Computing in Medicine and Life Sciences, University of Luebeck, Luebeck, Germany
[3] Institute for Anatomy, University of Luebeck, Luebeck, Germany
Email: hofmann@isip.uni-luebeck.de

Abstract— **Unified electro-optical microprobes for co-localized optical and electrical recordings within a rats brain have been recently introduced (Krapohl, Bonin et al. 2008). In this work, we show a simplified production method for these multimodal multisite neuroprobes. The electro-optical neuroprobe has an outer diameter of 255µm and is composed of eight NiChrome wires (Ø 25µm) fixed to the surface of a mono-mode glass fiber (Ø 125µm). Where the former method elaborately braids the wires around the fiber, the new method uses the property of a PTFE tube to shrink at higher temperature (>300°C). Thus the microwires are pressed to the fiber. The probe tip is than hand polished and is such ready to be used in rat brain navigation experiments, featuring both functions electrical as well as anatomical, optical look-ahead properties. The latter is achieved by using the glassfiber as working probe for an Optical Coherence Tomography (OCT) system. Hence these electro-optical probes are called OCTrodes. We determined the impedance of the OCTrodes by impedance spectroscopy to lie in the range of 500kΩ at 1kHz frequency. This range enables them to record both single and multi unit activity. OCT experiments have shown promising results in detecting transversal boundaries between structures of different density in phantoms and cadaver brain. Ongoing experiments aim at co-localized optical and electrical recordings in living animals.**

Keywords- Neural recording, OCTrode, Niotrode, multimodal neuroprobe, OCT.

I. INTRODUCTION

Deep brain targeting is even in the small animal not a trivial task, since interesting structures like the STN in a rat brain are of dimensions of some 100µm in an undisturbed brain [1]. This does not take into account dimpling effects due to probe insertion [2]. The situation worsens in human surgery due to man's bigger size and additional effects like brain shift [3-6]. Consequently, improved targeting in human DBS is achieved by adding intraoperative electrophysiological microelectrode recordings to pre-operatively achieved images [7-9], whereas rat stereotaxic surgery may benefit from better robotic stereotaxic frames [10,11]. To further improve this situation, at least in animal experiments, in situ navigation should be based on functional electrical as well as other properties of the tissue. Recent research showed that a method called Optical Coherence Tomography (OCT) is indeed applicable to image brain morphology at least ex vivo [12]. OCT-based identification of white matter has been demonstrated for perpendicular slices of rat brains in vitro [13,14]. We consequently proposed [15] to combine this intraoperative imaging modality in the very same microprobe with electro-physiological microelectrodes. The former would enable a look-ahead modality (like a flashlight) based on glass fiber OCT and the latter would enable functional multisite recordings in probes denominated OCTrodes. Within the current work, we present a simplification in the production process of the original artistically crafted multimodal OCTrodes and characterize them in vitro. In vivo experiments are currently under way. As shown in Fig. 1, an OCTrode is made of the multiple (eight) NiChrome wires pressed on the fiber core by a shrinking tube.

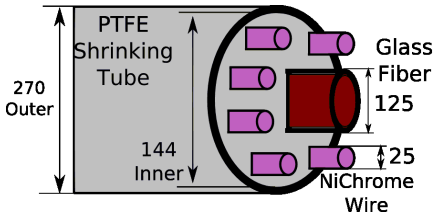

Fig. 1: Sketch of a multimodal multisite OCTrode. (All dimensions are in µm)

II. MATERIALS & METHODS

A. Simplified procedure

The original production of the OCTrode was based on a helical braiding process of microwires around either a center metal wire [16] or a glass fiber [15] (see Fig. 2).

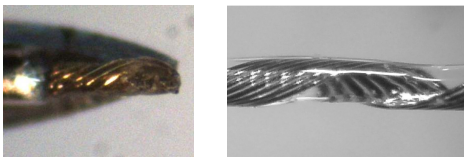

Fig. 2: original Niotrode (left) and original OCTrode (right).

An optical bank with a rotating jig and micromanipulators performed the task of wrapping eight microwires around the inner core. Epoxy coating adheres the microwires to the core and provides a smooth surface [15]. The new procedure simplifies this process significantly.

Instead of winding the microwires around the inner core (be it glass or metal), the core and the microwires are pulled effortlessly through a polytetrafluoroethene (PTFE, Teflon®) shrinking tube (Sublite-Wall, Zeus Inc., Orangeburg, USA) with an expanded inner diameter of 0.5mm. As shown in

Fig.3, in order to create tension and equal distribution on the front end of the probe, one end of each strand in the bundle is inserted into a hole in the wire guide and tightened to the adjacent small screw, the other ends are pulled through the shrinking tube and held by the wire holder. An inner core (Pt/Ir or glass fiber) takes the centre stance and is surrounded by eight NiChrome wires. The shrinking tube is dragged towards the wire guide and shrinking is performed by exposing the tube to a 300ºC hot airflow. The tubes inner diameter contracts to nominal 127µm and holds the bundle according to geometrical requirements. The diameter of the bundle yields 144µm, which confirms the tight fitting into the shrinking tube.

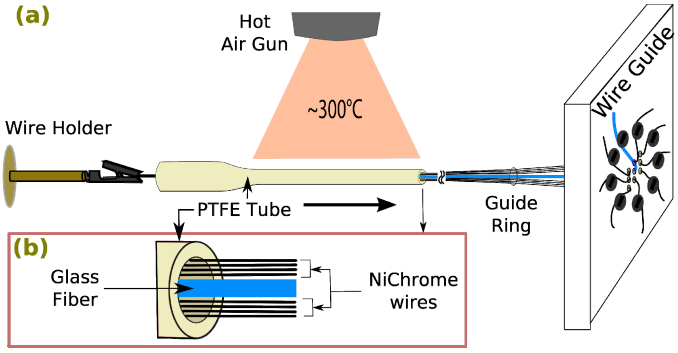

Fig. 3 : (a) A production setup of the OCTrodes (b) close view of the PTFE tube with inserted NiChrome wires and a monomode glass fiber

B. *Impedance characterization*

In order to characterize electrical properties of the probes and control manufacturing parameters, we utilized an impedance LCR meter (Instek LCR-800 series, GWInstek, Taiwan) in a three-point setup [17].

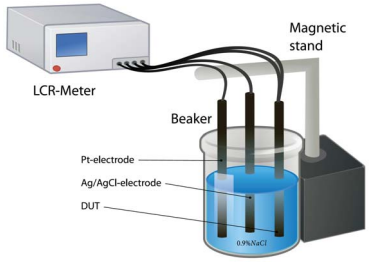

Fig. 4: Three point impedance measurement with counter, reference and working electrode immersed in electrolyte.

As shown in Fig. 4, four BNC-cables of equal length (750mm) were used to connect the electrodes to the interfaces of the LCR-meter. Three electrodes: an AgCl, a Platinum (Pt) and an OCTrode (DUT) are immersed into 0.9% NaCl saline at room temperature. To obtain impedance values and the phase angle, the LCR-meter is set to serial mode and a list of predefined frequencies to provide equidistant spacing on a logarithmic scale is subsequently entered.

C. *Niotrode*

As forerunner and procedural testbed for the mentioned OCTrodes a multiwire all-metal electrode (so called "Niotrode" [16]) was developed, which contains eight NiChrome wires. The inner core is a Pt/Ir wire (Ø 38µm). The production method remains the same as described earlier with the Pt/Ir wire as the centre of the bundle. An extra wire of Tungsten (76µm) may be used in the bundle for better packaging and increasing the overall diameter of the bundle. The front distribution of the wires is apparently not organized which was later resolved in the OCTrodes.

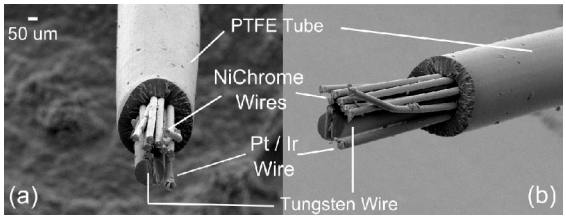

Fig. 5 : (a) & (b) An electron-micrograph of the Niotrode tip

D. *Optical phantom for brain tissue*

Since our primary goal for OCT use is to detect by A-scan modality layers and interfaces of the brain tissue ahead, we constructed phantoms to model some of the brains optical properties. These phantoms were made by stratifying gels of different physical densities (0.25%, 0.50% & 1% Agar-Agar in saline) in Petri dishes on top of each other (see Fig. 6). In order to increase the reflective properties in the material, an aluminum foil (13µm) was placed in the middle layer of agar (Fig. 6 (a)). In other two phantoms, aluminum foil was replaced by 2mm thick slice of tofu (bean curd) in the agar layers since the tofu visually resembles brain tissue. For ex vivo experiments on the tissue, the extracted rat brain was used by fixing it into the ice filled Petri dish with four needles [15].

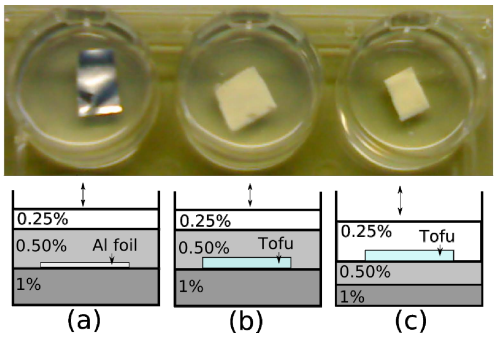

Fig. 6: The agar phantoms (a) with aluminum foil in the middle layer, (b) & (c) with tofu in the middle and top layers respectively

E. *OCTrode*

A bundle containing eight NiChrome wires (Ø 25µm) and a monomode glass fiber (Ø 125µm) is prepared to ca. 40cm length. After the outer tube shrinking procedure, 500µm length of the bundle in front of the shrinking tube is carefully cut under microscope inspection. To improve the front end stability and fixate the distribution of the microwires on the glass fiber, the bundle is fused by a drop of epoxy resin at the very tip. The front end of the bundle is finally polished by 5µm aluminum oxide lapping film (Thorlabs GmbH, Germany).

On the connecting end, wires and fiber are protected by shrinking tube until they split up in one branch leading to the electrical connector and another branch leading to the fiber

connector (see Fig. 7). Unglued ends of the microwires are passed through a protecting polyester tube, their coatings are removed and soldered to the contacts of a low profile mobile phone connector (AXR72161, Matsushita Electric Works, Ltd.) providing small contact resistance and high flexibility. The glass fiber leads to a FC/APC connector (Thorlabs GmbH, Germany) that plugs into the OCT device via an extension fiber.

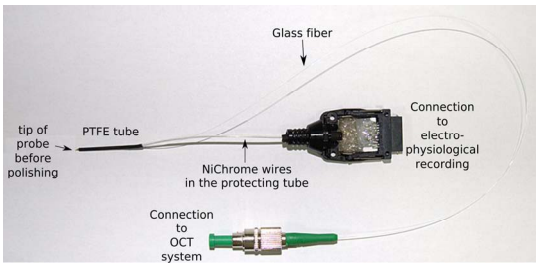

Fig. 7: An OCTrode assembly with its connectors

F. *Fiber OCT system*

As shown in the Fig. 7, the fiber connector plugs into a commercial OCT system ("Callisto", Thorlabs GmbH, Germany) (see Fig. 8). This OCT system is a Fourier domain OCT [18] enabling measurements with high sensitivity and high signal to noise ratio not un-like an Ultrasound A-scan. The system is connected to a computer by USB 2.0 interface. It performs the OCT procedure (essentially interference reflectometry) 1000 times per second by illuminating the tissue via the glass fiber in the core of OCTrode and displays the resulting image produced from the reflected light.

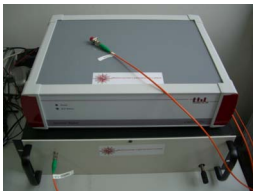

Fig. 8: The Callisto fiber OCT

III. RESULTS & DISCUSSION

A. *Electron Microscope Micrographs*

Wire bundles are routinely imaged by standard Raster Electron Microscope (Philips SEM 505, Philips, Netherlands) and show after polishing a smooth frontend, very much suitable for insertion. Unfortunately, the gold-plating for REM covers the NiChrome wire frontend (see Fig. 9). An OCTrode measures around 255µm diameter.

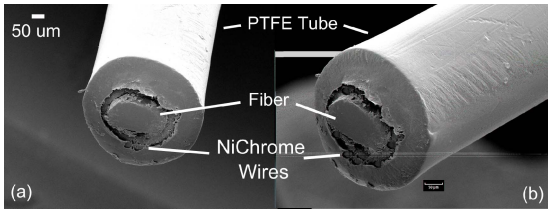

Fig. 9: REM micrographs of a typical OCTrode, covered with 30nm thick gold. The complete assembly's diameter here is 255µm

B. *Bundle electrode impedance*

The measured impedance values were plotted versus frequency with double logarithmic scaled axes. It can be seen that in double logarithmic scale the impedance decreases almost linearly with increasing frequency as predicted by theory [17]. It is also apparent that the impedance of the bigger Pt/Ir wire is far below the average impedance of the NiChrome wire, but also linear with frequency. With an impedance in the range of 500kΩ at 1kHz, we conclude that our procedure yield electrodes good enough to record multiple and single unit activity in brain tissue.

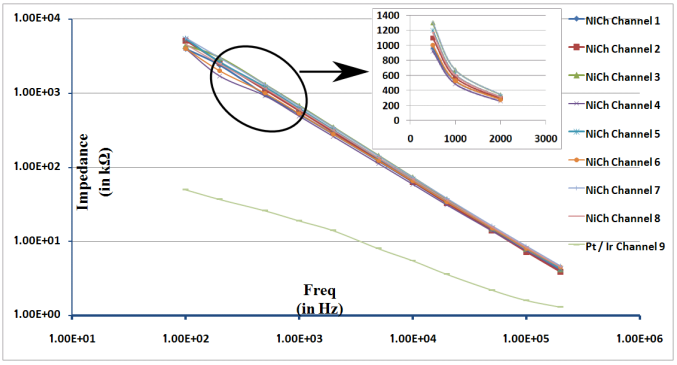

Fig. 10: Impedance of Niotrode microwires. Each of the nine wires was subsequently tested with the frequency range from 100 Hz – 200 kHz.

C. *OCT experiment with Agar phantom*

OCT measurements were performed with bare glass fibers of the same composition as the glass fiber used in the OCTrode. A robotic stereotaxy system [10] was used to guide the fiber probe into a phantom made of the different concentration layers of Agar (see in Fig. 6). The graphs in Fig.11 were obtained from the OCT with a sampling rate of 1000 A-scan per sec. Images were captured while the tip was moved towards the aluminium foil of phantom in Fig. 6(a). As the fiber approaches to the aluminium foil, the resulting reflection line in the image moves towards the base line (decreasing distance). Since the fiber can not physically penetrate the dense aluminium material, it starts to bend at the tip and thus captures less amount of backscattered light (visible in the decrease of amplitude).

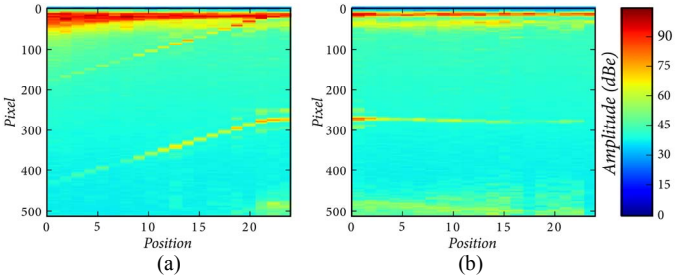

Fig. 11: The glass fiber was navigated in the agar phantom. (a) The aluminium foil is thus approaching towards the fiber tip. (b) The fiber can not penetrate the highly dense layer and looses the intensity due to bending at the tip.

In case of OCT measurements in rat brain, the glass fiber was navigated inside along the path shown in Fig. 12 (a) by dotted red line. The A-scans were captured at each 10 µm step.

Fig. 12(b) shows an A-scan OCT image captured at a particular point in the brain and manifests the detection of the boundaries at front of the fiber while the backscattered intensity fades away at the higher axial depth. The A-scan scenario can also be viewed in the graph (Fig. 12 (c)) which exhibits two sharp peaks of apparent boundaries within 0.5mm of penetration depth. Further image processing is required to improve visualization of OCT scans into brain tissue since the brain contains low contrast components which are difficult to detect.

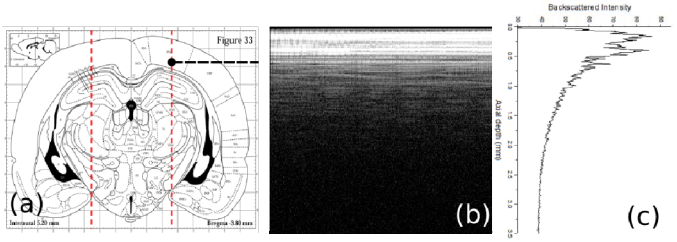

Fig. 12: (a) An atlas rat brain cross-section [1], (b) 1000 A-Scan image from the OCT system and (c) a graph of backscattered intensity vs. axial depth

IV. CONCLUSIONS

The previous production method of the OCTrode was very time consuming and difficult [15]. The described production in this work is not only simpler but also enables frontend improvements of the OCTrode by grinding and polishing. The OCTrode fiber succeeded to detect the boundaries between different density materials in a brain tissue phantom, but didn't fully succeed to do so in ex vivo brain tissue without further processing. The NiChrome wires used in our bundles have appropriate impedance for functional brain recording. Promising results have proved that OCTrodes exhibit recording enabling impedances and look ahead OCT property. This will make it possible to use them in deep brain targeting, which is currently work in progress.

V. ACKNOWLEDGMENT

The OCTrode project is funded under the innovation fund of the state of Schleswig-Holstein, Germany. We acknowledge support from the Institute for Biomedical Optics, Clinic for Neurology and the Institute for Robotics and Cognitive Systems, University of Luebeck.

REFERENCES

[1] Paxinos, G. and C. Watson (1998). The Rat Brain in Stereotaxic Coordinates, Academic Press.

[2] Knopp, U., W. Jensen, et al. (2004). Compression of the cerebral cortex during corticotomy: A study of dimpling in rats. 55. Ann' Jahrestagung der Deutschen Gesellschaft für Neurochirurgie, Köln, gms German Medical Sciences.

[3] Maurer, C. R., D. L. G. Hill, et al. (1998). "Investigation of intraoperative brain deformation using a 1.5-t interventional MR system: Preliminary results." IEEE Trans. on Medical Imaging 17(5): 817-825.

[4] Miga, M. I., K. D. Paulsen, et al. (1999). "Model-updated image guidance: Initial clinical experiences with gravity-induced brain deformation." IEEE Transactions On Medical Imaging 18(10): 866-874.

[5] Hastreiter, P., C. Rezk-Salama, et al. (2000). "Registration techniques for the analysis of the brain shift in neurosurgery." Computers & Graphics-UK 24(3): 385-389.

[6] Suess, O., T. Kombos, et al. (2002). "Impact of brain shift on intraoperative neurophysiological monitoring with cortical strip electrodes." Acta Neurochir 144: 1279-1289.

[7] Zonenshayn, M., A. R. Rezai, et al. (2000). "Comparison of anatomic and neurophysiological methods for subthalamic nucleus targeting." Neurosurgery 47(2): 282-294, ; discussion 292-4. Comment in: Neurosurgery. 2001 Aug;49(2):477.

[8] Menne, K. M. L., C. K. E. Moll, et al. (2004). "On-line 32 channel signal processing and integrated database improve navigation during cranial stereotactic surgeries." International Congress Series 1268 - CARS 2004: 443 - 448.

[9] Moll, C. K. E., A. Struppler, et al. (2005). "Intraoperative Mikroelektrodenableitungen in den Basalganglien des Menschen." Neuroforum 1: 11-20.

[10] Ramrath, L., U. G. Hofmann, et al. (2008). "A Robotic Assistant for Stereotactic Neurosurgery on Small Animals." Int. Journal on Medical Robotics and Computer Assisted Surgery 4(4):295-303.

[11] Ramrath, L., S. Vogt, et al. (2008). "Robot-Assisted Electrophysiological Brain Mapping:A feasibility study." in press Biomedizinische Technik / Biomedical Engineering.

[12] Boehringer, H.J., Giese, A., et al. (2006). "Noninvasive intraoperative optical coherence tomography of the resection cavity during surgery of intrinsic brain tumours" In 57. Jahrestagung der Deutschen Gesellschaft fuer Neurochirurgie, May 2006.

[13] Jeon, S.W., Rezai, A.R., et al.(2006). "A feasibility study of optical coherence tomography for guiding deep brain probe." Journal of Neuroscience Methods, 154:96–101, 2006.

[14] Jeon, S.W., et.al. (2005)."Optical coherence tomography and optical coherence domain reflectometry for deep brain stimulation probe guidance. In K.E. Bartels, editor, Photonic Therapeutics and Diagnostics. Proceedings of the SPIE, volume 5686, pages 487–494, 2005.

[15] Krapohl, D., T. Bonin, et al. (2008). "A new integrated optical and electrophysiological sensor." Biomed. Technik / Biomedical Engineering 53(Supp 1): 126-128.

[16] Gritsun, T., G. Engler, et al. (2007). A simple microelectrode bundle for deep brain recordings. 3rd Int'l Conference on Neural Engineering, Hawaii, USA, IEEE.

[17] Yoshida, K., Shruijk, J., The Theory of Peripheral Nerve Recording, Horch, K., Dhillon, G., Neuroprosthetics: Theory and Practice. 2004: vol. 2, World Scientific Publishing Co. Pte. Ltd.

[18] Bouma, B.E. and Tearney, G.J., Handbook Of Optical Coherence Tomography. 2002: Marcel Dekker Inc.